

Short-term forecasting of photovoltaic power generation

Abstract. In this article, a method for short-term forecasting of photovoltaic (PV) generation was proposed. The proposed method belongs to the group of physical methods and is based on numerical weather forecasts. The generation forecast was determined using the PV source model in the OpenDSS software. The results of calculations were compared with the results of measurements from the operating PV micro-installations.

Streszczenie. W artykule zaproponowana została metoda krótkoterminowego prognozowania generacji źródła fotowoltaicznego (PV). Metoda ta należy do grupy tzw. metod fizycznych i bazuje na numerycznych prognozach pogody. Do wyznaczenia prognozy generacji zastosowano model źródła fotowoltaicznego wchodzący w skład pakietu OpenDSS. Wyniki prognoz zostały porównane w wynikami pomiarów pochodzących z działających mikroinstalacji PV. (**Krótkoterminowe prognozowanie generacji źródła fotowoltaicznego**)

Keywords: photovoltaic source, prosumer, generation forecasting, physical method, numerical weather forecast, OpenDSS

Słowa kluczowe: źródło fotowoltaiczne, prosument, prognozowanie generacji, metoda fizyczna, numeryczna prognoza pogody, OpenDSS

Introduction

The increasing power of renewable energy sources [1], especially prosumer photovoltaic (PV) micro-installations [2], changes the operating conditions of the power grid. Distribution system operators are increasingly reporting emerging problems in the operation of the low-voltage (LV) grid. These problems mainly concern an increase in voltage above the permissible limit, the appearance of the reverse power flow from the LV network to the medium-voltage (MV) network, an increase in voltage asymmetry, and a higher load of some network elements. The described phenomena occur locally, in places where a large number of PV micro-installations have been connected [3]. The risk of exceeding the normal operating conditions of the LV network increases as the power of PV sources increases [4].

Excessive power of PV sources connected locally to the LV grid also affects the situation of prosumers, especially during periods of high solar irradiation, when they produce the majority of the energy. Due to the low demand that usually occurs at this time, most of the energy produced is transmitted to the grid. This raises the voltage at the prosumer's connection point. Once the voltage exceeds the permissible limit, the inverter turns off and no energy is produced despite favorable weather conditions. As a result, the prosumer suffers a measurable loss. The situation described is illustrated in Figure 1.

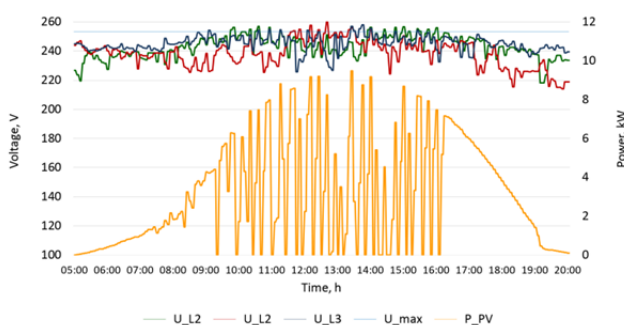


Fig. 1. Phase voltages and power generated by a PV micro-installation belonging to one of the authors of the article (measurements from May 15, 2022; visible interruptions in production caused by switching off the inverter due to exceed the voltage limit)

The standard method to improve the operating conditions of the LV grid with connected PV micro-installations is its modernization. Modernization usually consists in increasing the power of the MV/LV transformer and the cross sec-

tion of the conductors, as well as shortening the LV circuits [5]. However, this is a costly method and takes a long time to implement the investment. An alternative solution is to increase the consumption of energy at the place where it is generated, at the same time as this generation occurs, i.e., to increase self-consumption. This can be achieved by appropriate control of selected household electrical appliances owned by the prosumer and using energy storages, connected in the prosumer's power supply system [6]. Proper determination of the operating schedule of these devices during the day requires a forecast of the generation of the PV source.

Numerous studies have reviewed various PV power forecasting methodologies [7-11]. These works classify PV power forecasting mainly depending on the forecasting horizon and methods used to forecast. The duration of time for which the forecasting of the PV power output is performed is called the forecasting horizon [8, 10]. Based on the time horizon, forecasting of PV power generation can be generally divided into three categories: long-term (done from one month to several years), medium-term (done for more than one week to one month), and short-term (done for one hour, several hours, one day or up to seven days). Long-term forecasts are used to plan the development of electricity generation, transmission, and distribution. Medium-term forecasts are important for planning the maintenance of power plants and networks in a cost-effective way. Short-term forecasts of PV generation are useful in unit commitment and dispatching of electrical power, as well as in scheduling of spinning reserves and demand response. These types of forecasts are also helpful in designing a PV integrated energy management system for buildings.

There are two main methods used for forecasting PV generation, namely statistical and physical [7, 9, 11]. Statistical approach consists in predicting the power output using historical data. Therefore, the quality of the data is essential for an accurate forecast. Statistical methods require a large historical dataset (meteorological and power measurements) to correctly define the correlation among them. The selection of a suitable training dataset becomes crucial for the accuracy. The statistical approach includes artificial neural networks, support vector machines, Markov chain, autoregressive, and regression models. Statistical models do not need any technical information from the PV system to model them. In contrast, the second approach, i.e., physical methods (also known as PV performance models), uses analytical equations and technical data to model the PV system. These methods use forecasted meteorological data

to calculate PV production. The main advantage of physical methods over the statistical methods is that no historical data are needed. However, the major disadvantage of these models is the high dependence on weather forecast, especially the forecast of solar irradiance. Physical methods include numerical weather forecasts, sky imagery, and satellite-imaging models.

In this article, we propose a physical method for short-term forecasting of a PV generation, based on numerical weather forecasts. We determine the generation forecast using the PV source model in the OpenDSS software. We compare the results of the calculations with the results of measurements from the operating PV micro-installations.

Model of a PV source

The PV source model used by OpenDSS [12] is presented in Figure 2 [4]. To parameterize the model, we first define the rated power of the PV panels $P_{r,PV}$ under standard test conditions. The power generated by the PV panels is determined for a given level of solar irradiance and is dependent upon the panel temperature, so the obtained power value must be corrected accordingly. The temperature of the PV panels is calculated using an external model based on ambient temperature, solar irradiance intensity, and wind speed. The DC power generated P_{DC} is then converted according to the efficiency characteristic of the inverter, for which the rated power S_r , the rated voltage U_r , and the power factor pf are given. The active power P and the reactive power Q generated by the PV source are calculated at the output of the inverter.

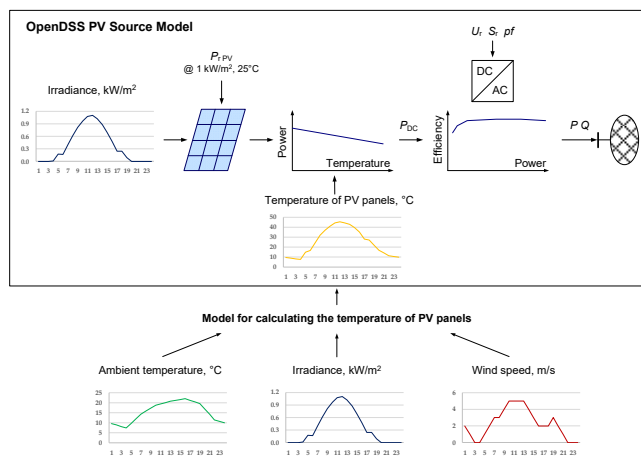


Fig. 2. The PV source model used by OpenDSS [4]

In the following part of the article, the PV source model will be validated using the measurements for the PV installation operating at the Silesian University of Technology.

The PV micro-installation at the Silesian University of Technology (SUT)

The SUT PV micro-installation is located on the roof of the building of the Faculty of Automatic Control, Electronics and Computer Science (Fig. 3). This building is equipped with three PV installations. Installation no. 3 was selected for the tests, because in the other two there was periodic shading of the PV panels by building elements. The selected installation is characterized by the same angle of inclination and orientation of all panels towards the cardinal directions. The installation consists of 66 NeMo 60 P modules with a rated power of 265 W, which gives a total installed power of 17.49 kW. It is based on the SolarEdge system, consisting of 33 power optimizers (P600) and an inverter (SE17K) with a rated power of 17 kVA.

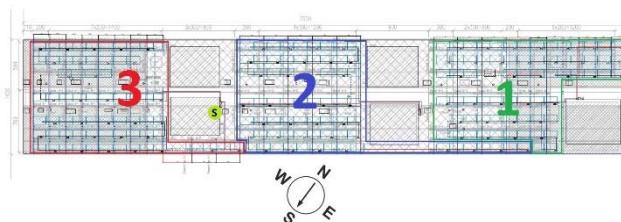


Fig. 3. PV installation on the roof of the building of the Faculty of Automatic Control, Electronics, and Computer Science of the Silesian University of Technology in Gliwice, Poland

Adjacent to the PV installation, there is a weather station measuring ambient temperature and wind speed. The weather station is also equipped with an external temperature sensor for PV temperature measurement. The solar irradiance is measured with a pyranometer. The PV installation is equipped with a SCADA (Supervisory Control And Data Acquisition) system that records the weather conditions and generated power with an one-minute resolution.

Weather conditions during the selected days

Two random days from 2021 were selected for the analysis. These days differed primarily in the intensity of solar irradiation. The first day, June 27, was a sunny day with temporary clouds. The second day, September 29, was cloudy with varying degrees of cloud cover. The weather conditions on selected days are illustrated in Figures 4 and 5. These figures also show the recorded temperature variability of the PV panels.

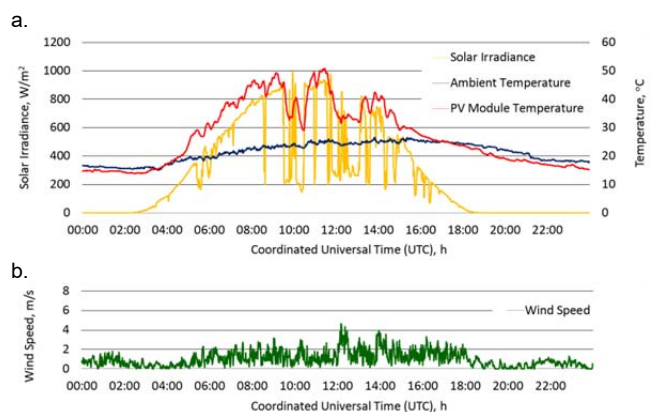


Fig. 4. Solar irradiance, ambient temperature, PV module temperature (a), and wind speed (b) on June 27, 2021

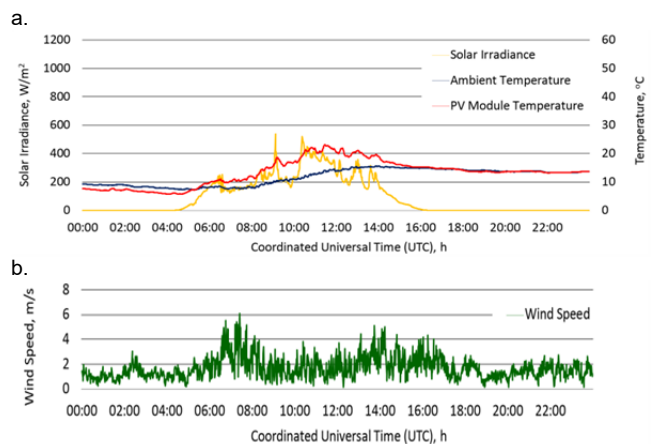


Fig. 5. Solar irradiance, ambient temperature, PV module temperature (a), and wind speed (b) on September 29, 2021

Correction of solar irradiance

Figures 4a and 5a show the measured intensity of solar irradiation falling on a horizontal surface. On this basis, the intensity of solar irradiation incident on the surface of PV modules, that are inclined to the horizontal at an angle of 12° and tilted from the north-south axis by 35° in the eastern direction, was determined. The calculations used a procedure according to PN-EN ISO 52010-1:2017-09, as described in the article [13]. Parameters that define the position of the sun relative to the PV panels were determined using the NOAA Solar Calculator [14]. Figures 6 and 7 compare the measured and corrected solar irradiance. The corrected solar irradiance will be used to calculate the generation of PV panels.

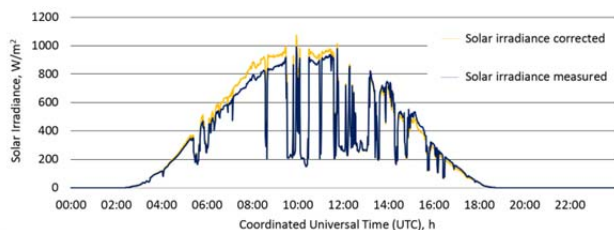


Fig. 6. Solar irradiance on sloped surface (corrected) vs. solar irradiance on a horizontal surface (measured) on June 27, 2021

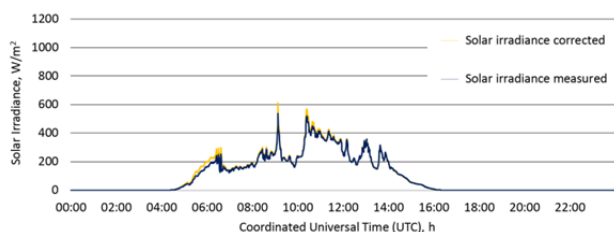


Fig. 7. Solar irradiance on sloped surface (corrected) vs. solar irradiance on a horizontal surface (measured) on September 29, 2021

Estimation of the PV module temperature

The operating temperature of the PV panel has a direct influence on power output. As the temperature increases, power generation decreases. The power temperature coefficient for PV panels in considered micro-installation was equal to 0.42%/°C. This means that a 10°C increase in temperature results in a 4.2% reduction in generated power. In the article, a dynamic thermal model proposed in [15] was used to determine the temperature of PV panels. This model is based on the finite difference method and uses data on ambient temperature, solar irradiation, and wind speed. The measured and calculated daily variation of PV panels temperature is shown in Figures 8 and 9. The temperature estimation error did not exceed 9°C on June 27 and 5°C on September 29.

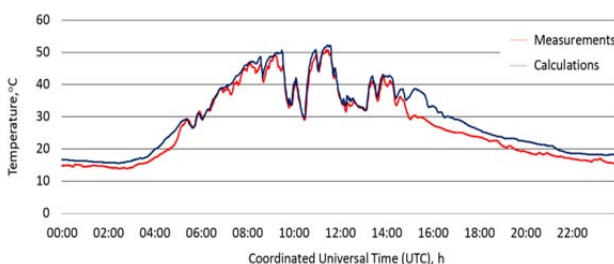


Fig. 8. Temperature of a PV module calculated using the finite difference model vs. measured temperature – atmospheric conditions on June 27, 2021

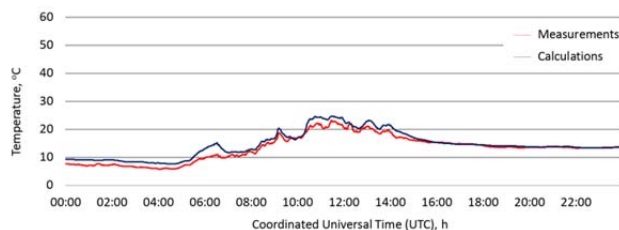


Fig. 9. Temperature of a PV module calculated using the finite difference model vs. measured temperature – atmospheric conditions on September 29, 2021

Validation of the PV source model

The PV source model was parameterized according to the technical data for the analyzed SUT PV micro-installation. Subsequently, corrected solar irradiance (Figures 6 and 7) and calculated PV panel temperature (Figures 8 and 9) were entered into the model. On this basis, the generation of the micro-installation was calculated for the two days analyzed. The results of the calculation were compared with the generation measured on those days. The results are presented in Figures 10 and 11.

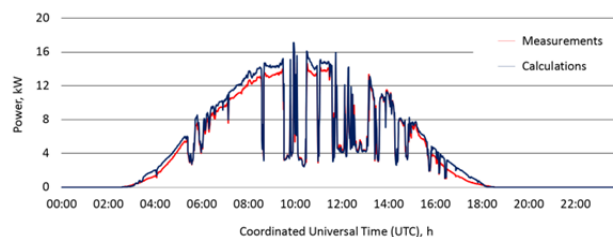


Fig. 10. Generation of PV installation calculated using the PV source model vs. measured power – atmospheric conditions on June 27, 2021

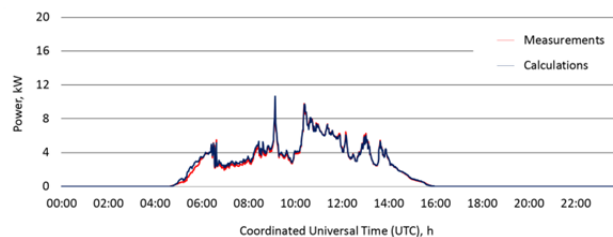


Fig. 11. Generation of PV installation calculated using the PV source model vs. measured power – atmospheric conditions on September 29, 2021

Comparing the results obtained using the PV source model with the measurements (Figs. 10 and 11), a high accuracy of estimation of the PV generation can be observed. The quality of PV model can be evaluated applying the mean absolute percentage error (MAPE) defined as:

$$(1) \quad MAPE = \frac{1}{n} \sum_{t=1}^n \left| \frac{P_m(t) - P_c(t)}{P_m(t)} \right| \cdot 100\%$$

where: $P_m(t)$ – measured PV generation at time interval t , in kW, $P_c(t)$ – calculated PV generation at time interval t , in kW, n – the total number of time intervals in analyzed period (1440). The values of MAPE errors for both days analyzed, as well as the measured and calculated amount of a daily energy production, are given in Table 1.

Table 1. Daily energy production and MAPE

Day	Daily energy production			MAPE
	Measured	Calculated	Difference	
	kWh	kWh	%	%
June 27	98.6	105.9	7.4	18.6
September 29	38.5	39.8	3.4	8.7

The applied model of the PV source turned out to be less accurate for a day with a higher level of solar irradiance. An in-depth analysis of the results allowed us to conclude that the largest difference between the measured and calculated PV generation occurs for the morning hours (up to 6.00) and the afternoon hours (after 16.00). If only hours from 6.00 to 16.00 are considered for the assessment of the model accuracy (approximately 90% of the daily energy is generated during this period), the error values are significantly smaller (see Table 2).

Table 2. Energy production and MAPE – hours from 6.00 to 16.00

Day	Daily energy production			MAPE
	Measured	Calculated	Difference	
	kWh	kWh	%	
June 27	87.3	91.8	5.2	6.8
September 29	36.9	37.8	2.3	4.9

The described model can also be used to determine the forecasted generation of the PV source. For this purpose, numerical weather forecasts should be used as input to the model.

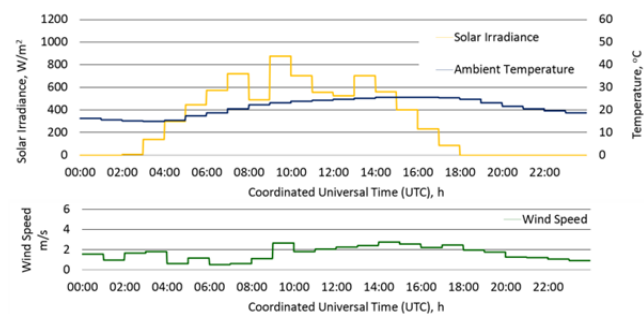


Fig. 12. Numerical weather forecast from the platform A for June 27, 2021 (hourly resolution)

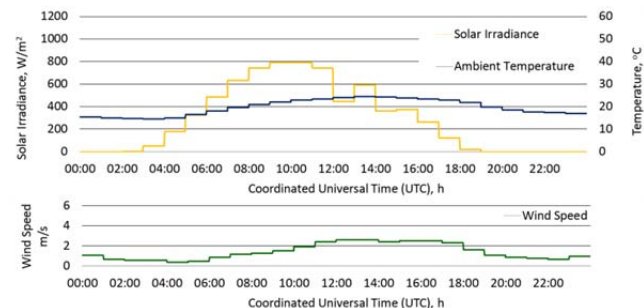


Fig. 13. Numerical weather forecast from the platform B for June 27, 2021 (hourly resolution)

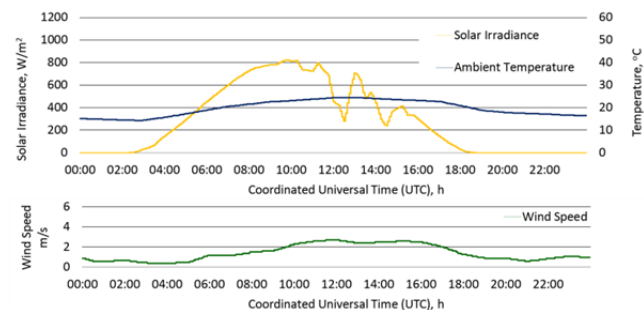


Fig. 14. Numerical weather forecast from the platform B for June 27, 2021 (5 minute resolution)

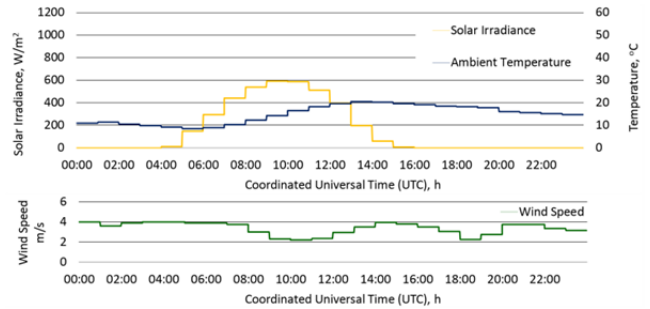


Fig. 15. Numerical weather forecast from the platform A for September 29, 2021 (hourly resolution)

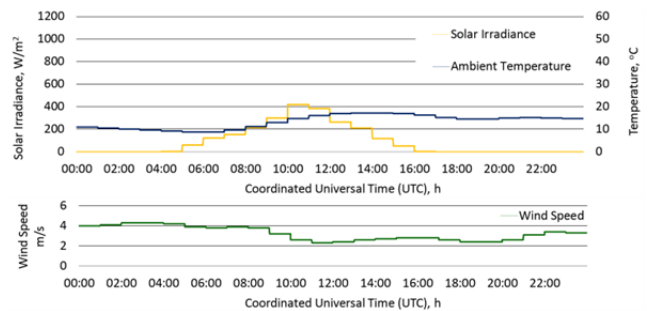


Fig. 16. Numerical weather forecast from the platform B for September 29, 2021 (hourly resolution)

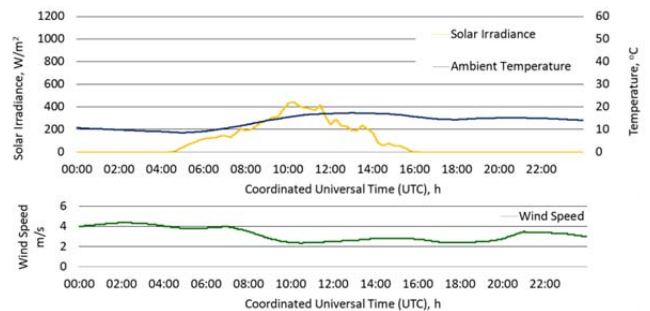


Fig. 17. Numerical weather forecast from the platform B for September 29, 2021 (5 minute resolution)

Numerical weather forecasts

The numerical weather forecasts used in the calculations came from two internet platforms (A and B). Both platforms provide information about the forecasted ambient temperature, wind speed, and solar irradiation through the API (application programming interface). The geographic resolution for platform A is 4 km and for platform B is 2 km. Platform A allows to download data in hourly resolution, while platform B in hourly and five-minute resolution. The weather forecasts from both platforms for the two days analyzed in the article are shown in Figures 12-17.

PV generation forecasts

Using the procedure described in the previous sections, and based on the numerical weather forecasts presented in Figures 12-17, appropriate forecasts of the generation of the PV source with an installed capacity of 17.49 kW were determined. The calculation results are shown in Figures 18-23 and Table 3.

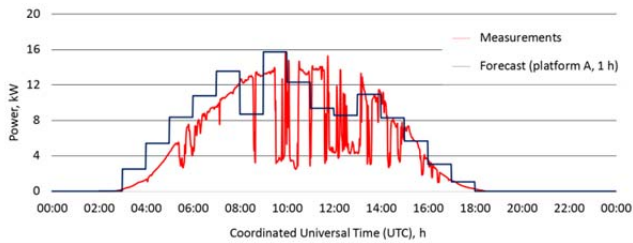


Fig. 18. Forecast of PV generation based on the platform A weather forecast (1 h) vs. measured power on June 27, 2021

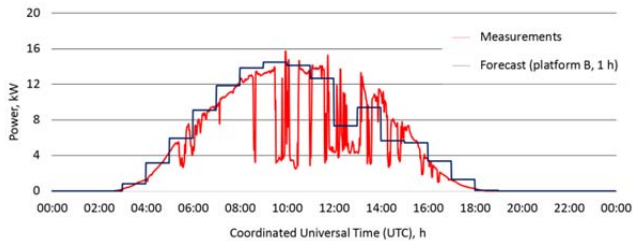


Fig. 19. Forecast of PV generation based on the platform B weather forecast (1 h) vs. measured power on June 27, 2021

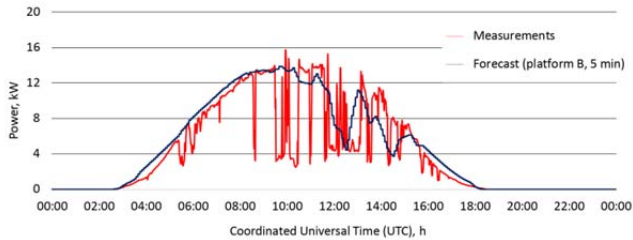


Fig. 20. Forecast of PV generation based on the platform B weather forecast (5 min) vs. measured power on June 27, 2021

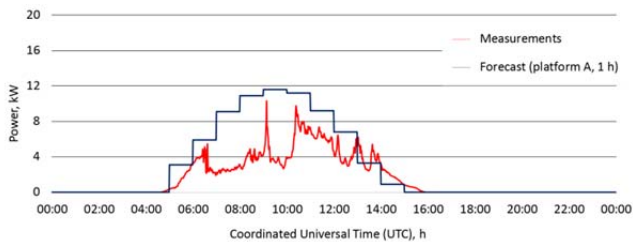


Fig. 21. Forecast of PV generation based on the platform A weather forecast (1 h) vs. measured power on September 29, 2021

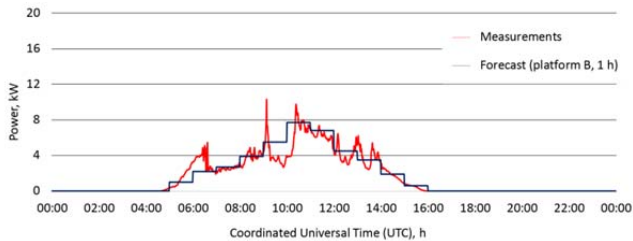


Fig. 22. Forecast of PV generation based on the platform B weather forecast (1 h) vs. measured power on September 29, 2021

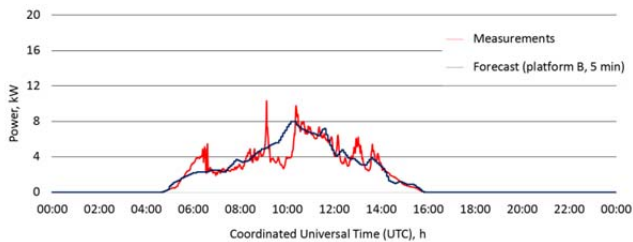


Fig. 23. Forecast of PV generation based on the platform B weather forecast (5 min) vs. measured power on September 29, 2021

Table 3. Forecast of daily energy production and MAPE

Day	Platform, resolution	Daily energy production			MAPE
		Measured kWh	Calculated kWh	Difference %	
June 27	A, 1 h	98.6	124.5	26.3	87.1
	B, 1 h		118.3	20.1	59.7
	B, 5 min		114.2	15.9	53.4
September 29	A, 1 h	38.5	72.0	86.9	124.7
	B, 1 h		40.3	4.6	28.5
	B, 5 min		39.9	3.6	26.5

The obtained generation forecasts differ from the actual production of the analyzed PV source. The accuracy of the forecasts is different for both the days considered and for different numerical weather forecasts. The forecasts obtained for the numerical weather forecasts from platform A are characterized by the lowest accuracy. The highest accuracy was obtained for platform B weather forecasts with a five-minute resolution. In the best case, the difference between the forecast and the actual generation was 3.6%, and the MAPE error did not exceed 27%.

In the following section, weather forecasts in five-minute resolution from platform B will be used to forecast the generation of prosumer micro-installations.

Generation forecast for a prosumer PV installations

The developed method was used to calculate the generation forecast for two prosumer micro-installations. The first is located in Koszęcin (Silesian Voivodeship). It is a household PV installation with an installed power of 7.32 kW. The installation consists of 24 IBC Solar PV panels with a power of 305 W and a Fronius Symo 6.0-3M inverter with a rated power of 6 kW. In the analyzed installation, the panels face south-west and are inclined at an angle of 35°. The forecast was developed using the numerical weather forecast for June 10, 2022 (Fig. 24). The results are shown in Figure 25 and Table 4.

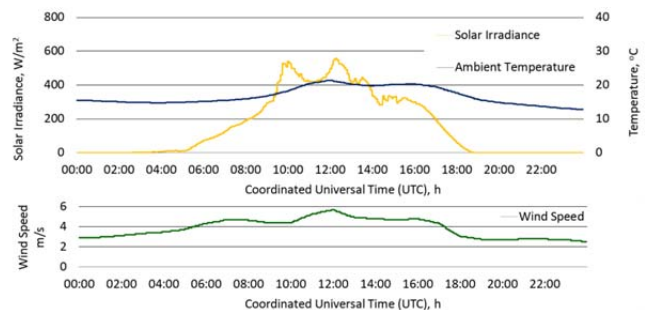


Fig. 24. Numerical weather forecast from the platform B for June 10, 2022 (5 minute resolution)

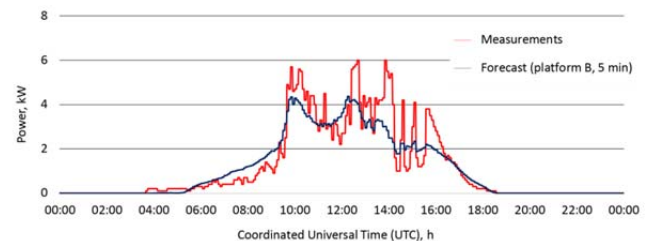


Fig. 25. Forecast of PV generation based on the platform B weather forecast (5 min) vs. measured power on June 10, 2022

Table 4. Daily energy production and MAPE

Day	Daily energy production			MAPE
	Measured kWh	Calculated kWh	Difference %	
June 10	28.4	26.5	-6.8	43.1

The second micro-installation is located in Łącza (Silesian Voivodeship). The installation consists of 20 LONGI Solar LR6-60PE modules with a rated power of 305 W, which gives a total power of 6.1 kW. The panels are connected to the Fronius Symo 5.0-3M inverter with a rated power of 5 kW. In the analyzed installation, the panels face south and are inclined at an angle of 15°. The forecast was prepared for June 16, 2022, also using the numerical weather forecast from platform B in a five-minute resolution (Fig. 26). The calculation results are shown in Figure 27 and Table 5.

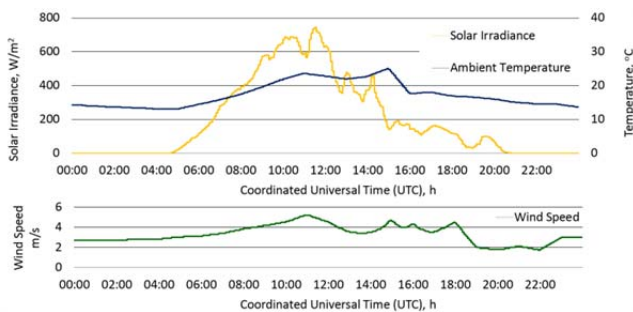


Fig. 26. Numerical weather forecast from the platform B for June 16, 2022 (5 minute resolution)

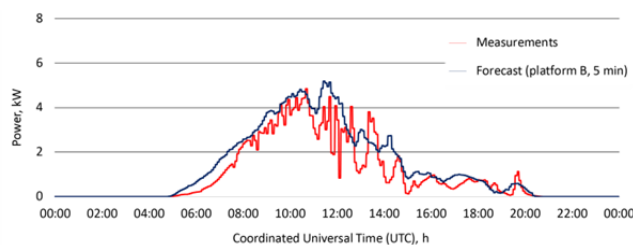


Fig. 27. Forecast of PV generation based on the platform B weather forecast (5 min) vs. measured power on June 10, 2022

Table 5. Daily energy production and MAPE

Day	Daily energy production			MAPE
	Measured kWh	Calculated kWh	Difference %	
June 16	23.9	30.8	28.7	70.0

Conclusions

The article presents a method of forecasting the generation of a PV source using numerical weather forecasts including the forecast of solar irradiation, ambient temperature, and wind speed. The possibility of using hourly and five-minute weather forecasts from two meteorological platforms was analyzed. The results of the forecasts were compared with the actual generation of three operating PV micro-installations.

The accuracy of PV generation forecasts depends on the source of the numerical weather forecasts and their resolution, as well as on the nature of the weather on the analyzed day, in particular on the nature of cloud cover. In the article, days with highly variable cloudiness were selected for analysis. From the point of view of forecasting the generation of a PV source, these are days for which forecasting is very difficult. The analyzes performed indicate that much higher accuracy was obtained for weather forecasts with a five-minute resolution. This type of PV source generation forecast is characterized by sufficient accuracy

to be used to determine the operating schedule of the selected household electrical appliances and energy storages owned by prosumers in order to increase the self-consumption of the produced energy.

Autorzy: dr hab. inż. Roman Korab prof. PŚ; E-mail: roman.korab@polsl.pl, Politechnika Śląska, Katedra Elektroenergetyki i Sterowania Układów, ul. B. Krzywoustego 2, 44-100 Gliwice; mgr inż. Tomasz Kandzia, Politechnika Śląska, Wydział Elektryczny, absolwent 2022, E-mail: tomaszkandzia@protonmail.com; mgr inż. Tomasz Naczyński – Politechnika Śląska, Wspólna Szkoła Doktorów, doktorant; E-mail: tomasz.naczynski@polsl.pl;

LITERATURA

- [1] pse.pl/dane-systemowe/funkcjonowanie-kse/raporty-roczone-z-funkcjonowania-kse-za-rok/raporty-za-rok-2021 (in Polish)
- [2] ptpiree.pl/energetyka-w-polsce/energetyka-w-liczbach/mikroinstalacje-w-polsce (in Polish)
- [3] Topolski Ł., Schab W., Flirt A., Piątek K.: Analysis of the impact of dispersed generation on selected aspects of power quality in a low-voltage electricity network located in the area of energy cluster Virtual Green Ochotnica Power Plant. *Przeгляд Elektrotechniczny*, vol. 3 (96), 2020, doi: 10.15199/48.2020.03.05 (in Polish)
- [4] Korab R., Połomski M., Smółka M.: Evaluating the Risk of Exceeding the Normal Operating Conditions of a Low-Voltage Distribution Network due to Photovoltaic Generation. *Energies* 2022, 15, 1969, doi:10.3390/en15061969
- [5] Adamek S.: Methods to reduce adverse impact of prosumer microinstallations on LV distribution systems. *Rynek Energii*, vol. 6 (163), 2022 (in Polish)
- [6] Naczyński T., Korab R.: Possibilities of forming the electricity balance of an individual customer equipped with a photovoltaic source. *Przeгляд Elektrotechniczny*, vol. 11 (97), 2021, doi:10.15199/48.2021.11.38 (in Polish)
- [7] Antonanzas J., Osorio N., Escobar R., Urraca R., Martinez-de-Pison F.J., Antonanzas-Torres F.: Review of photovoltaic power forecasting. *Solar Energy*, vol. 136, 2016, doi:10.1016/j.solener.2016.06.069
- [8] Das U.K., Tey K.S., Seyedmahmoudian M., Mekhilef S., Idris M.Y.I., Van Deventer W., Horan B., Stojcevski A.: Forecasting of photovoltaic power generation and model optimization: A review, *Renewable and Sustainable Energy Reviews*, vol. 81, part 1, 2018, doi:10.1016/j.rser.2017.08.017
- [9] Sobri S., Koochi-Kamali S., Rahim N.A.: Solar photovoltaic generation forecasting methods: A review. *Energy Conversion and Management*, vol. 156, 2018, doi:10.1016/j.enconman.2017.11.019
- [10] Akhter M.N., Mekhilef S., Mokhlis H., Shah N.M.: Review on forecasting of photovoltaic power generation based on machine learning and metaheuristic techniques. *IET Renewable Power Generation*, 2019, 13, doi:10.1049/iet-rpg.2018.5649
- [11] Wu Y.K., Huang C.L., Phan Q.T., Li Y.Y.: Completed Review of Various Solar Power Forecasting Techniques Considering Different Viewpoints. *Energies* 2022, 15, 3320, doi:10.3390/en15093320
- [12] EPRI: OpenDSS PVSystem Element Model. Version 1. February 23, 2011. www.epri.com/pages/sa/opensdss
- [13] Michalak P.: Modelling of solar irradiance incident on building envelopes in Polish climatic conditions: the impact on energy performance indicators of residential buildings. *Energies* 2021, 14, 4371. https://doi.org/10.3390/en14144371
- [14] NOAA Solar Calculator, gml.noaa.gov/grad/solcalc/index.html
- [15] Korab R., Połomski M., Naczyński T., Kandzia T.: A dynamic thermal model for a photovoltaic module under varying atmospheric conditions. *Energy Conversion and Management*, vol. 280, 2023, doi.org/10.1016/j.enconman.2023.116773